International Journal of Mass Spectrometry 304 (2011) 140–147

Contents lists available at ScienceDirect

International Journal of Mass Spectrometry

journal homepage: www.elsevier.com/locate/ijms

Gas-phase ion/ion reactions of rubrene cations and multiply charged DNA and RNA anions

Teng-yi Huang, Scott A. McLuckey*

Department of Chemistry, Purdue University, 560 Oval Drive, West Lafayette, IN 47907-2084, USA

ARTICLE INFO

Article history:
Received 1 April 2010
Received in revised form 18 June 2010
Accepted 21 June 2010
Available online 26 June 2010

Keywords:
Negative electron transfer dissociation
Nucleic acid anions
Ion/ion reactions

ABSTRACT

Gas-phase ion/ion reactions between multiply deprotonated DNA and RNA anions and rubrene radical cations have been investigated in this research. Ion/ion reactions of DNA 6-mer (dT_6, dC_6, dA_6 and dG_6) anions with rubrene radical cations led to negative electron transfer dissociation (nETD), complex formation, and negative electron transfer without dissociation (nET no D). The amount of nET, no D product (G > A > C > T) is inversely related to nucleobase ionization potential (G < A < C < T). On the other hand, the amount of complex formation (G < A < C < T) is positively related to the nucleobase ionization potential, with only minimal complex formation being observed for dG_6. The nETD channels generally led to the generation of w/d- and a•/z•-ions, but were only observed when highly deprotonated precursor ions were reacted. Similar trends were observed when reacting RNA 8-mer (rU_8, rC_8, rA_8 and rG_8) anions with rubrene radical cations (i.e., the yields of nET, no D products (G > A > C > U) and complex formation (G < A < C < U) are inversely related to one another). The major nETD product ions were w/d-ions and a•/z•-ions, as with the DNA anions, and were only observed at relatively high precursor ion charge states. Furthermore, extensive fragmentation from the w/d- and a•/z•-ion channels can be obtained from simultaneous activation of the first generation nET, no D survivor radical anions (nET-CID). In comparison to the conventional collisional activation methods, the dissociation of DNA and RNA anions via either nETD or nET-CID is less affected by the structural differences on the 2′-hydroxyl group of the sugar ring.

1. Introduction

Although the major constituents of genetic material are relatively few (i.e., dA, dT, dG and dC for DNA, and rA, rU, rG and rC for RNA), there exist various types and extents of sequence variants from cellular modifications or mutagen damage, which can affect biological function. Compared to other conventional sequencing methods, tandem mass spectrometry of relatively small oligonucleotides is rapid and sensitive; therefore, it has been widely used for sequencing and structural characterization of natural and chemically modified oligonucleotides [1–3]. In addition, probing nucleic acid higher order structure using tandem mass spectrometry-based methods has also been demonstrated [4].

Due to the highly acidic phosphodiester linkage between nucleotides, it is common to ionize oligonucleotides in negative ion mode via electrospray ionization (ESI). The gas-phase dissociation of oligonucleotide anions is usually conducted using collision induced dissociation (CID) or infrared multiphoton dissociation (IRMPD) [5–10]. Dissociation of DNA anions is initiated by loss of neutral or charged base, followed by subsequent 3′C–O bond cleavage [5,6]. The resulting complementary a-B/w-ions provide sequence information. However, the product ion spectra from CID of DNA anions tend to be highly influenced by nucleobase identity because the propensity for base loss is nucleobase-dependent. Dissociation of RNA anions via collisional activation in the gas-phase leads to 5′ P–O backbone bond cleavage, which gives rise to the characteristic c/y-ion series [11,12]. This dissociation channel is initiated from the formation of an intramolecular cyclic intermediate through the bridging between the 2′-OH hydrogen and the 5′ phosphate oxygen. Abstraction of the 2′-OH proton by the 5′ oxygen then leads to the dissociation of the 5′ P–O bond [12]. This cleavage mechanism, which is relatively insensitive to nucleobase identity, competes with nucleobase loss and the subsequent backbone cleavage to yield (a-B)/w-ion series [13]. The characteristic ions from both c/y- and (a-B)/w-ion series can provide primary sequence information and allow the identification of the presence of modified nucleosides [14].

Gas-phase dissociation of biopolymer ions under different activation conditions or via distinct dissociation methods often results in unique dissociation phenomena that can provide complementary structural information. Since the introduction of electron-based dissociation methods for biopolymer analysis, such

* Corresponding author. Tel.: +1 765 494 5270; fax: +1 765 494 0239.
E-mail address: mcluckey@purdue.edu (S.A. McLuckey).

1387-3806/$ – see front matter © 2010 Elsevier B.V. All rights reserved.
doi:10.1016/j.ijms.2010.06.019

as electron capture dissociation (ECD) [15–18] and electron transfer dissociation (ETD) [19–21], many applications have been demonstrated in the characterization of multiply charged cations derived from peptides and proteins. ECD and ETD of oligonucleotide cations have also been demonstrated [22,23]. ECD of multiply protonated DNA generates radical cations and low abundant product ions from various backbone bond cleavages, with w/d-ions being the most prominent. On the other hand, ECD of multiply protonated RNA generates very limited sequence information. For ETD, reaction of multiply protonated DNA cations with fluoranthene radical anions leads to efficient electron transfer charge reduction and limited backbone cleavage to yield sequence ions of low abundance [24]. Subsequent CID of the charge-reduced oligonucleotide radical cations (ETcaD) generates a/w- and d/z-ion series. In comparison to CID of the even electron ions, the abundances of base loss ions and internal fragments are significantly lower. ETcaD of an oligonucleotide duplex resulted in specific backbone cleavages, rather than dissociation into single strands.

Due to the relative ease of generating oligonucleotide anions via ESI, it is desirable to explore alternative methods that might be applicable for oligonucleotide anion characterization. For example, it has been shown that radical DNA anions can be generated from multiply deprotonated DNA via electron detachment resulting from 240 to 290 nm UV irradiation. The electron photodetachment yield is inversely related to the ionization potential of nucleobases, which suggests that the detachment of the electron is initiated at the bases rather than the phosphates. When the resulting DNA radical anions are subjected to CID, w-, d-, a$^{\bullet}$- and z$^{\bullet}$-ions are observed, in addition to neutral losses. This dissociation method has been coined as electron photodetachment dissociation (EPD) [25,26]. Dissociation methods analogous to ECD and ETD have also been demonstrated for the analysis of oligonucleotide anions via ion/electron reactions (electron detachment dissociation, EDD) and ion/ion reactions (negative electron transfer dissociation, nETD). For EDD [27–30], multiply deprotonated DNA and RNA anions were subjected to high energy electron irradiation (i.e., 15–20 eV), which led to DNA and RNA backbone bond cleavage in the gas-phase. The dissociation behavior varied among different oligonucleotides. The w- and d-type ions are generally the most prominent fragment ions for both DNA and RNA, while other dissociation channels are also observed. In contrast with irradiation with 240–290 nm photons, no nucleobase-dependence was reported for EDD, suggesting, perhaps, that the energies of the electrons were sufficiently high to detach electrons from the various oligomers with similar efficiencies. However, no charge state effects on the reaction phenomenology have been investigated systematically for the two methods. For nETD [31–33], ion/ion reactions of multiply deprotonated DNA anions with various reagent radical cations, such as $Xe^{+\bullet}$, CCl_3^+, $O_2^{+\bullet}$, has also been demonstrated, which led to the generation of DNA radical anions and sequence specific fragment ions, a/w-ion series, complementary to that afforded by CID. In comparison to CID, the cleavage of the N-glycosidic bond is significantly decreased; therefore, fewer base loss ions are observed.

In this work, a systematic study of the gas-phase reaction of the rubrene (5,6,11,12-tetraphenylnaphthacene) radical cation with multiply charged anions of both DNA and RNA has been conducted. Rubrene cations were generated using nano-ESI and used as a novel electron transfer reagent. The only other reagent cations formed via ESI used to date to extract an electron from multiply charged anions have been derived from transition metal complexes, such as the copper (II) bis- and tris-phenanthroline cations. Reactions of doubly charged transition metal complexes with multiply deprotonated 5′-d(AAAAAA)-3′ [34] and triply deprotonated peptide DGAILDGAILD [35] have been examined. However, transition metal ion transfer into the anion is a major competing channel and can be the dominant reaction pathway, depending upon anion charge state, transition metal, and the extent of metal ion coordination. Hence, rubrene was chosen for this study to avoid the possibility for metal ion transfer. The extent of dissociation noted in conjunction with electron transfer from a multiply charged anion is directly related to the recombination energy of the reagent cation. Recombination energies are equal to the ionization energies of the corresponding neutrals, provided the same electronic states are involved in the ionization of the neutral and the neutralization of the ion. The ionization energies for Xe, CCl_3, O_2, and rubrene are 12.1, 8.1, 12.1, and 6.4 eV [36]. Hence, the rubrene cation is expected to be a relatively soft electron transfer reagent.

2. Experimental

2.1. Materials

The DNA 6-mers (dA_6, dT_6, dG_6 and dC_6), DNA 12-mer (dCAGAGCGCCAAG) and RNA 8-mers (rA_8, rU_8, rG_8, rC_8 and rUCGCACCA) were custom synthesized by Integrated DNA Technologies (Coralville, IA). Piperidine, imidazole, ammonium acetate, ethanol, and rubrene were obtained from Sigma-Aldrich (St. Louis, MO). Methanol, isopropanol, dichloromethane and glacial acetic acid were purchased from Mallinckrodt (Phillipsburg, NJ). All DNA and RNA samples were re-suspended in water to a concentration of 100–200 μM as a stock solution without further purification. The oligonucleotide solutions for negative nano-electrospray were prepared by diluting the aqueous stock solutions to ca. 20–40 μM in 20/80 (v/v) isopropanol/water with addition of 25 mM piperidine and 25 mM imidazole. The reagents were dissolved in dichloromethane to a concentration of ca. 4 mM and then diluted to ca. 80 μM in 20/80 (v/v) dichloromethane/acetonitrile [37].

2.2. Apparatus and procedures

All experiments were performed using a prototype version of a QqTOF tandem mass spectrometer modified to allow for ion/ion reaction studies [38]. A home-built pulsed dual nano-ESI source was coupled to the nanospray interface to produce ions of both polarities [39]. The oligonucleotide samples and the reagent solutions were loaded into two separate nano-electrospray emitters pulled from borosilicate capillaries (1.5 mm o.d., 0.86 mm i.d.) using a P-87 Flaming/Brown micropipet puller (Sutter Instruments, Novato, CA). A stainless steel wire was inserted into the back of each capillary, and a potential of 0.8–1.1 kV was applied to the wire for ionization. Both the multiply deprotonated oligonucleotides, $[M-nH]^{n-}$, and the reagent radical cations were generated directly via the nano-ESI emitters. For negative electron transfer ion/ion reactions (nET) to take place, Q1 selected precursor ions were injected into Q2 at a relatively low kinetic energy and then reacted with the reagent cations in the Q2 collision cell. To perform nET-CID, a dipolar rf signal with frequency in resonance with the fundamental secular frequency of the electron transfer charge-reduced radical product ions (nET, no D ions) was then applied to one pair of the Q2 rods to induce ion trap CID during the course of ion/ion reactions. The fragment ions were then subjected to mass spectrometry analysis by TOF.

3. Results and discussion

3.1. Ion/ion reactions of rubrene radical cation with DNA and RNA

Multiply deprotonated DNA anions were subjected to ion/ion reactions with ESI-generated rubrene cations. As shown in Fig. 1,

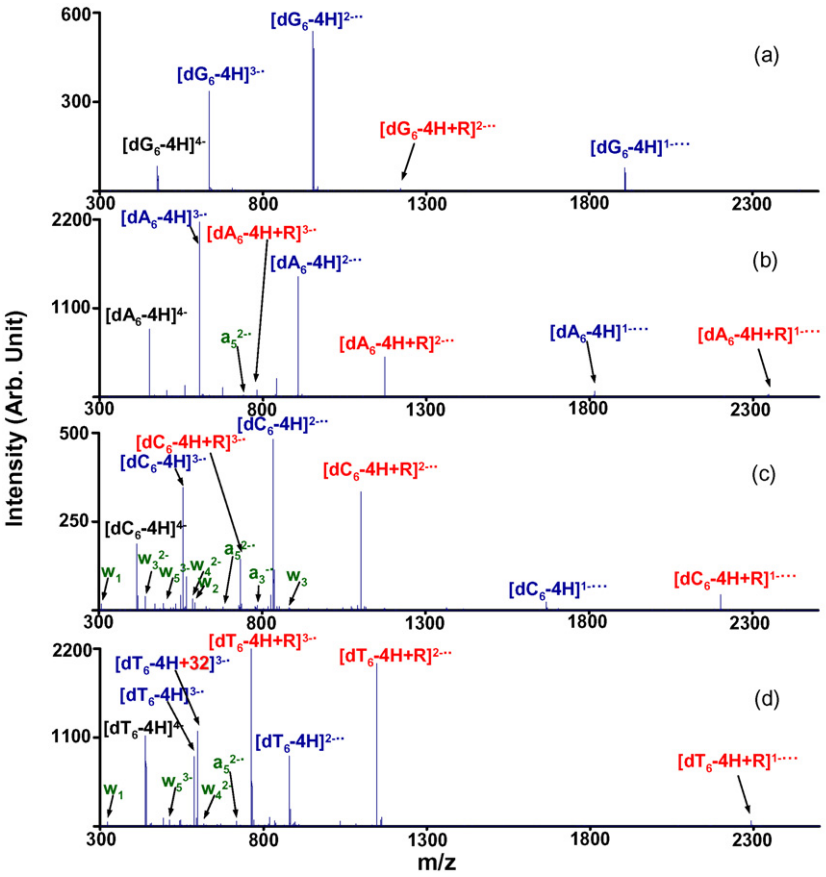

Fig. 1. Ion/ion reactions of DNA 6-mers with rubrene radical cations. The $[M-4H]^{4-}$ ions of (a) dG_6, (b) dA_6, (c) dC_6 and (d) dT_6 were reacted with rubrene (R) radical cations generated via nano-ESI.

ion/ion reaction of the $[M-4H]^{4-}$ ions of four model DNA 6-mers (dT_6, dC_6, dA_6 and dG_6) with rubrene radical cations led to negative electron transfer without dissociation (nET, no D), complex formation, and negative electron transfer dissociation (nETD) to varying degrees. The reaction channel partitioning is nucleobase-dependent. For the nET, no D channels, the relative abundances of the observed nET, no D charge-reduced radical product ions (G > A > C > T) are inversely related to the ionization potential of nucleobases (G < A < C < T), in analogy with the electron photodetachment studies [25,26]. The tendency for complex formation, on the other hand, shows the opposite trend (viz., (G < A < C < T)) with only minimal complex formation being observed for dG_6. No particular nucleobase-dependent trend was noted for the smaller reagent cations ($Xe^{+\bullet}$, CCl_3^+, $O_2^{+\bullet}$) and neither was reagent cation attachment observed.

The two major nucleobase-dependent trends mentioned above are consistent with the current understanding of ion/ion reaction dynamics for large multiply charged ions [40]. The relevant processes that give rise to products are indicated in Scheme 1. The ET, no D product from electron transfer can arise either from a direct electron transfer at a crossing point on the energy hypersurface or via the break-up of a relatively long-lived ion/ion collision complex intermediate. The attachment products are simply stabilized ion/ion collision complexes. When the complexes were subjected to collisional activation, by far the dominant dissociation channel was the loss of neutral rubrene to yield the $[M-nH]^{n-\bullet}$ ion for all of the oligomers that showed adduct formation (data not shown). Hence, the abundances of the two types of products are expected to be inversely related.

As indicated in Scheme 1, there are two pathways to formation of the ET, no D product. It is not possible from these data alone, however, to determine the relative contributions of these two pathways. Plausible explanations can be offered for the nucleobase-dependence for the partitioning between complex formation and electron transfer for each of the pathways. On one extreme, it might

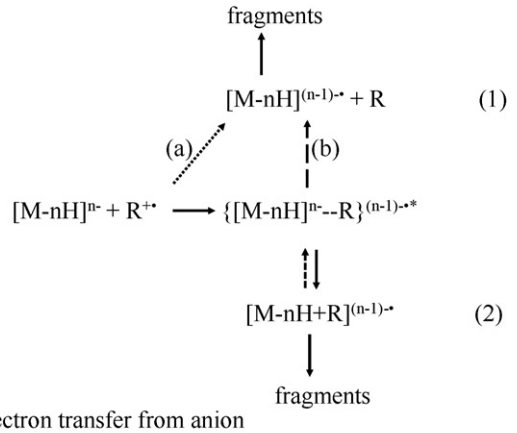

(1) Electron transfer from anion
  (a) Electron transfer at a crossing point
  (b) Electron transfer via complex
(2) Cation/anion attachment

Scheme 1. A summary of the major processes relevant to the reaction of multiply charged DNA or RNA anions ($[M-nH]^{n-}$) with ionized rubrene, R = $C_{42}H_{28}$.

be argued that all electron transfer occurs via formation of the long-lived complex intermediate, as represented in Scheme 1 as pathway 1(b) (i.e., no electron transfer at a crossing point without complex formation), and that the partitioning between electron transfer and complex formation reflects the relative stabilities of the complexes to rubrene loss. In other words, the partitioning would reflect directly the competition between pathway 1(b) and pathway (2). This interpretation would lead to the conclusion that rubrene loss is most facile for the complex with dG_6 and least facile for the complex comprised of dT_6. The fact that collisional activation of the complexes in all cases leads to rubrene loss as the strongly dominant process suggests that rubrene is bound to the nucleic acid anions via non-covalent bonding. The relatively high polarizability of the polynuclear aromatic hydrocarbon is expected to facilitate binding with the anions. The strength of the ion-induced dipole interaction would not be expected to differ significantly for the various nucleobases for a given anion charge state. Neither is it obvious that the strength of possible interactions with the nucleobases would follow the order G < A < C < T. However, the relative thermodynamic stabilities of the $[M-nH]^{(n-1)-\bullet}$ ions are expected to contribute to the height of the barrier for rubrene loss. This would suggest that the $[M-nH]^{(n-1)-\bullet}$ anion of dG_6 is the most stable of the group and that for dT_6 is least stable.

The other limiting interpretation is that all electron transfer products are formed via electron transfer at a crossing point without the formation of the long-lived complex (pathway 1(a)) and that all collisions that lead to a complex (i.e., all sticky collisions) result in the observation of a complex (pathway (2)). This interpretation assumes no pathway 1(b). The partitioning between electron transfer and complex formation in this interpretation is determined by the relative magnitudes of the cross-section for electron transfer at a crossing point and the cross-section for a sticky collision [34]. Of course, scenarios intermediate to the two extremes just mentioned that involve varying degrees of processes 1(a), 1(b), and 2 may apply. There is strong evidence from the work relating the reactions of dA_6 anions with transition metal complex cations that process 1(a) can make major contributions to the product partitioning [34]. That work showed that complex formation resulted in metal ion transfer so that the partitioning between processes 1(a) and 2 could be quantified. There is no compelling evidence to suggest that the cross-section for an intimate collision differs significantly for anions of dG_6, dA_6, dC_6, and dT_6. However, the results of the electron photodetachment studies [25,26], which show a strong inverse relation between nucleobase ionization energy and propensity for electron detachment, suggest that there could be significant differences in the electron transfer cross-section. The locations of the crossing-points for transfer of an electron from a nucleobase to the cation on the energy hypersurface are dependent upon the nucleobase ionization energy such that the relative probabilities for process 1(a) could differ substantially for the various nucleobases. Unfortunately, only anions of dA_6 were subjected to reaction with the transition metal complex cations. Examination of anions comprised of the other nucleobases in reaction with transition metal complex cations could shed further light on this issue.

Direct nETD, represented by the processes that lead to fragments in Scheme 1, comprised a relatively small fraction of product partitioning in Fig. 1 and was most apparent for the anions of dC_6 and dT_6. In comparison to CID of DNA, in which the (a-Base)- and w-ions are usually observed, the nETD channels generally lead to the generation of w/d- and $a^\bullet$/$z^\bullet$-ions. Due to the palindromic sequence of the model oligonucleotides, it is not possible to distinguish the w-ions from the d-ions and the $a^\bullet$-ions from the $z^\bullet$-ions. It is interesting that most direct nETD was noted for the anions of dC_6 and dT_6 and that very little was noted for anions of dA_6 and even less for anions of dG_6. This could reflect a greater propensity for fragmentation of the dC_6 and dT_6 anions. An alternate hypothesis, however, can be proposed based on energy partitioning. The initial potential energy associated with the separated oppositely charged ions can be partitioned between relative translation of the products as well as internal energies of the products. In the case of electron transfer at a crossing point, much of the relative translation of the reactants can remain as translation in the products. In the case of complex formation, however, all of the relative translational energy is converted into internal energy of the long-lived complex. Hence, the $[M-nH]^{(n-1)-\bullet}$ ions generated via processes 1(a) and 1(b) may well have different internal energies. In this interpretation, greater degrees of fragmentation are associated with anions that go through the long-lived complex, such as the dC_6 and dT_6 anions, due to a greater extent of translational-to-internal energy conversion associated with long-lived complex formation.

The other noteworthy observation associated with the phenomena apparent in Fig. 1 is the relatively extensive attachment of molecular oxygen to the $[M-4H]^{3-\bullet}$ ion of dT_6 (see the peak labeled $[M-4H+32]^{3-\bullet}$ in Fig. 1(d)). The oxygen is present as a minor component of the gas (mostly nitrogen) in the reaction cell used to translationally cool the ions. Attachment of molecular oxygen to radical peptide cations [41], radical peptide anions [35], and radical anions of dA_6 [34] generated via ion/ion electron transfer has been noted in this instrument. The results reported here show that the extent to which oxygen attachment takes place with

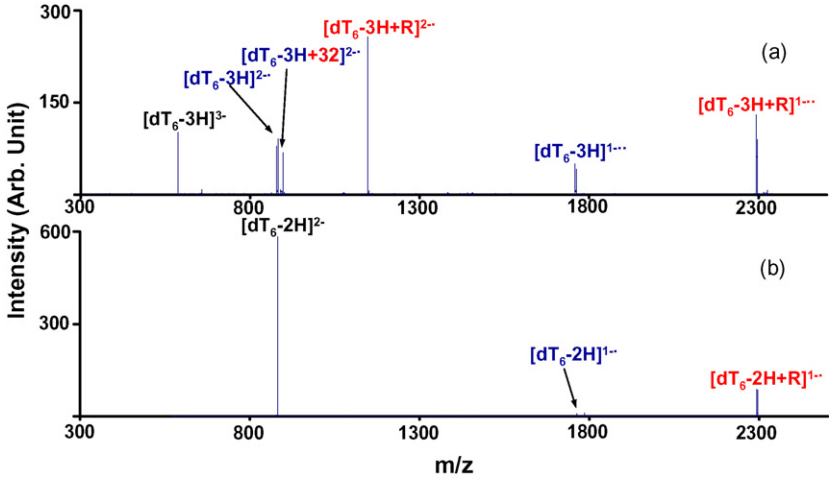

Fig. 2. Ion/ion reactions of the (a) $[M-3H]^{3-}$ and (b) $[M-2H]^{2-}$ of dT_6 with rubrene (R) radical cations generated via nano-ESI.

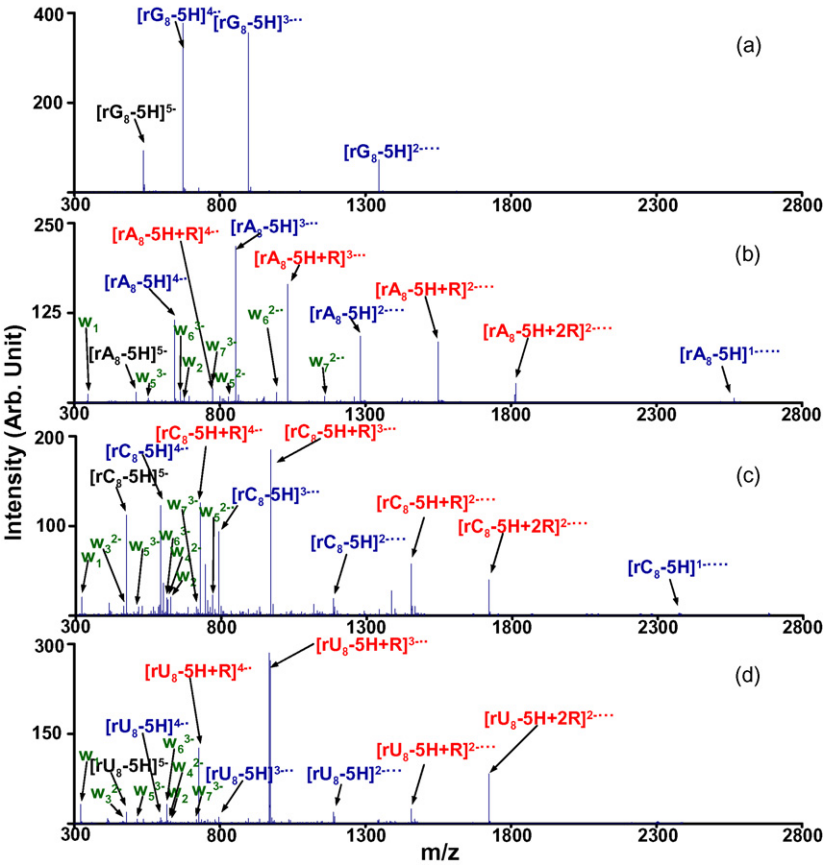

Fig. 3. Ion/ion reactions of RNA 8-mers with rubrene radical cations. The $[M-5H]^{5-}$ ions of (a) rG_8, (b) rA_8, (c) rC_8 and (d) rU_8 were reacted with rubrene radical cations generated via nano-ESI.

oligonucleotide radical anions is nucleobase-dependent. In particular, attachment to poly-T appears to be favored over attachment the other homopolymer anions (both RNA and DNA) or the mixed base RNA oligomers. Although O_2 adduct signals can be identified in some of the data collected for oligomers lacking T, they are usually only a few percent of the signal associated with the non-adducted species. Thymine peroxyl radical has been observed before, and the mechanisms as well as their possible biological effects, such as the formation of tandem lesions, have been proposed [42,43]. Despite the structural similarity between thymine and uracil, no +32 ions were observed for the charge-reduced radical anions of uridine-containg RNA 8-mers (see below). These results taken collectively suggest that the electron lost from the reactive poly-T anions likely originates from the nucleobase and that the radical thymine is more reactive to oxygen than the other nucleobases.

The 3- and 2- charge states of the four DNA 6-mers have also been subjected to ion/ion reactions with rubrene radical cations. Similar nucleobase-dependent tendencies for electron transfer versus complex formation were noted for all charge states (i.e., electron transfer followed the order G > A > C > T and rubrene cation attachment followed the order T > C > A > G). The data for dT_6 are provided here for illustration. Fig. 2 shows the results for the 3- (Fig. 2(a)) and 2- (Fig. 2(b)) charge states while the results for the 4-charge state are given in Fig. 1(d). In general, the relative contribution of electron transfer tends to decrease with the absolute charge of the anion and complex formation increases correspondingly. The difference is most notable in comparing the data for the 3- anion with that for the 2- anion. Only the 4- charge state showed measurable nETD for dT_6 (see Fig. 1(d)). This was also the case for the dC_6 and dA_6 systems. The absence of direct nETD for the lower charge states might be attributable to lower overall reaction exothermicity as the anion charge decreases and perhaps due to increased kinetic stability of the product anion as the charge state decreases due to lower electrostatic repulsion in the $[M-nH]^{n-\bullet}$ product.

The major structural difference between RNA and DNA is the substitution of a hydroxyl group on the 2′ position of the ribose ring of RNA. This substitution not only affects the geometry of DNA and RNA in solution, but also affects their dissociation behavior under vibrational activation conditions in the gas-phase. While structural characterization of RNA by itself is an important research topic, the parallel comparison of a dissociation method for sequencing both types of genetic materials may provide mechanistic information explaining the reaction phenomenology. To this end, ion/ion reactions of RNA 8-mer homo-oligomer anions with rubrene radical cations were also carried out. In comparison to the DNA 6-mers, ions of higher charge states were observed for the RNA 8-mers. As shown in Fig. 3, the ion/ion reaction product partitioning from reaction of the 5-precursor ions of RNA 8-mer (rU_8, rC_8, rA_8 and rG_8) anions with rubrene radical cations was very similar to those of DNA anions. Three major reaction channels were observed, namely nET, no D, complex formation and nETD. The relative abundances of the nET, no D product ions for the four RNA 8-mers (G > A > C > U) are inversely correlated to the ionization potential of the nucleobases (G < A < C < U). The relative abundances of the complex formation product ions (G < A < C < U) are positively correlated to the ionization potential of the nucleobases (G < A < C < U). The similarity in the trends for the DNA and RNA anions with respect to electron transfer and complex formation suggest that the presence or absence of the 2′-OH group on the sugar plays no significant role in determining the ion/ion electron transfer behavior. The ion/ion reaction

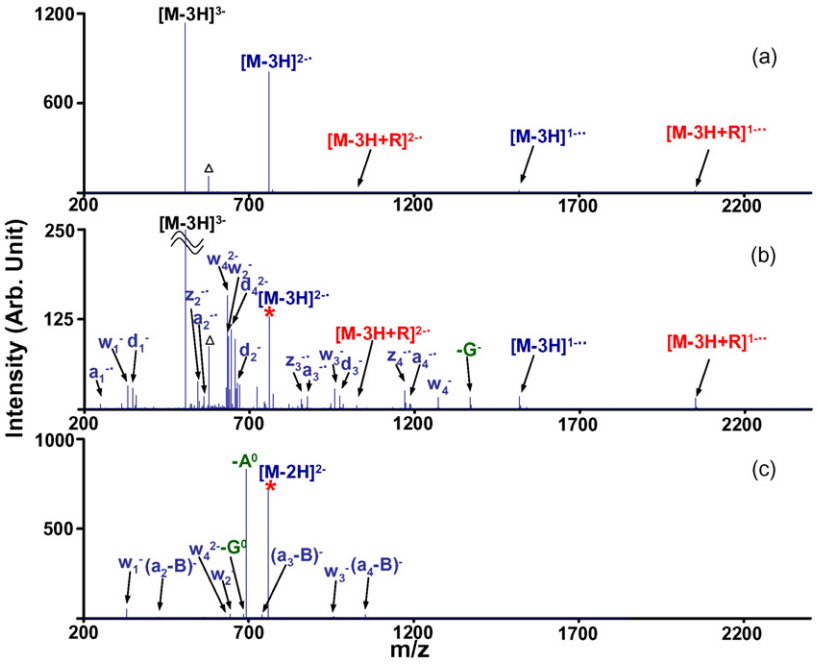

Fig. 4. Comparison of product ion spectra from (a) ion/ion reactions of the $[M-3H]^{3-}$ ions of a DNA 5-mer, dGAAAA, with rubrene radical cations; (b) simultaneous activation (115 kHz, 400 mV) of the $[M-3H]^{2-\bullet}$ survivor ions during ion/ion reactions; (c) ion trap CID of the $[M-2H]^{2-}$ DNA 5-mer ions (115 kHz, 400 mV).

results for rubrene cations and RNA and DNA anions appear to be much more similar to electron photodetachment than to electron detachment. The ion/ion reaction, at least with the relatively low recombination energy reagent rubrene cation, shows selectivity reminiscent of UV photodetachment. Sequence information can also be derived directly from low abundance nETD product ions. The major nETD product ions observed were w/d-ions and a•/z•-ions, and were also only observed at higher precursor ion charge states. No characteristic CID fragment ions (c/y-ions) were observed.

3.2. Collisional activation of the survivor ions (nET-CID) during ion/ion reaction

Based on the results presented above, direct nETD with rubrene cations is limited to precursor ions of relatively high charge states. However, the selection of very high charge state precursor ions can lead to complications in sequencing because of the generation of complicated product ion spectra from consecutive reactions. For lower charge state ions, generally no sequence information can be obtained due to the lack of direct nETD. A general strategy to increase the yield of peptide cation fragmentation from electron transfer or electron capture experiments is to activate the survivor ions after the electron transfer/capture events or to activate the precursor ions prior to ion/ion or ion/electron reactions. By prior or subsequent energy deposition via gas-phase activation, dissociation can be facilitated. To effect dissociation, resonance excitation of the first generation nET, no D survivor radical anions was conducted during the ion/ion reactions. That is, a resonance excitation frequency tuned for the charge-reduced $[M-nH]^{-\bullet}$ product was applied during the ion/ion reaction period.

Figs. 4 and 5 compare the tandem mass spectra from ion/ion negative electron transfer reactions, collisional activation of the first generation survivor ions, and the conventional collisional activation of anions of a DNA 5-mer (dGAAAA) (Fig. 4) and anions of a RNA 5-mer (rGAAAA) (Fig. 5). As shown in Figs. 4a and 5a, no nETD fragment ions were observed from ion/ion reactions of the $[M-3H]^{3-}$ ions of the DNA and RNA 5-mers; predominantly charge-reduced ions via negative electron transfer and low abundant complex ions were observed. When the first generation $[M-3H]^{2-\bullet}$ radical anions were subjected to ion trap CID during the ion/ion reaction period (Figs. 4b and 5b), full sequence coverage was obtained for both DNA and RNA 5-mers from abundant a•/w-ion series and d/z•-ion series from cleavage of the 3′ C–O and 5′ O–C backbone bonds. While ion trap CID of the $[M-2H]^{2-}$ ions of the DNA and RNA 5-mers showed the characteristic a-B/w-ion series for DNA and c/y-ion series for RNA (Figs. 4c and 5c), very similar dissociation patterns were observed for the DNA and RNA radical ions under collisional activation. The observations indicate that the introduction of a radical site significantly affects the gas-phase dissociation of DNA and RNA. In addition, the dissociation of DNA and RNA under nETD and nET-CID conditions is less sensitive to the presence of the 2′-hydroxyl group on the ribose in comparison to conventional CID.

To demonstrate the general applicability of nETD/nET-CID for sequencing small DNA and RNA oligomers, a DNA 12-mer (dCAGAGCGCCAAG) (Fig. 6) and an RNA 8-mer (rUCGCACCA) (Fig. 7) were used as model systems. As shown in Fig. 6, the $[M-7H]^{7-}$ ion of the DNA 12-mer reacted primarily via electron transfer and, to a lesser degree, by adduct formation (see Fig. 6(a)). The relatively high guanosine content likely plays a key role in favoring electron transfer. The high G content may also be a factor in the absence of nETD fragmentation. However, when the first generation $[M-7H]^{6-\bullet}$ radical anions were subjected to ion trap CID during ion/ion reaction (Fig. 6b), extensive fragmentation was observed. One of the most favorable dissociation channels is cleavage of the glycosidic bond to generate charged base loss ions ($-A^-$ and $-G^-$). However, no significant evidence for the subsequent dissociation of these base loss ions (e.g., the relevant a-B ions) were observed. In comparison to ion trap CID of the $[M-6H]^{6-}$ ion (Fig. 6c), where base loss ions (both charged and neutral base losses) and the a/a-B/w-ions dominated in the spectrum, the nET-CID generated abundant a•/w- and d/z•-ion series.

The nETD and nET-CID spectra of relatively low charge state mixed-residue RNA anions have also been compared with the ion

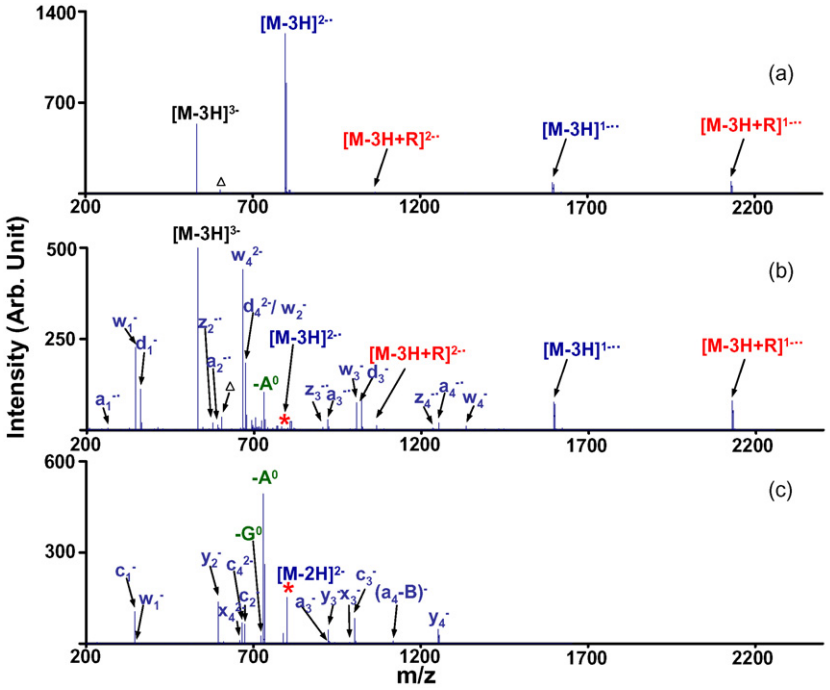

Fig. 5. Comparison of product ion spectra from (a) ion/ion reactions of the $[M-3H]^{3-}$ ions of a RNA 5-mer, rGAAAA, with rubrene radical cations; (b) simultaneous activation (109 kHz, 400 mV) of the $[M-3H]^{2-\bullet}$ survivor ions during ion/ion reactions; (c) ion trap CID of the $[M-2H]^{2-}$ RNA 5-mer ions (109 kHz, 400 mV).

trap CID spectra. As shown in Fig. 7a, ion/ion reaction of $[M-3H]^{3-}$ of an RNA 8-mer (rUCGCACCA) with rubrene radical cations led to charge reduction via either nET, no D or complex formation. The abundance of the complex is lower than the nET, no D product and no nETD fragment ions were observed. The subsequent collisional activation of the $[M-3H]^{2-\bullet}$ radical anions led to the generation of abundant neutral loss ions (loss of neutral guanine, adenine, cytosine, 168 and 206 Da neutrals), w- and d-ion series and sporadic a•/a-B•-/y-ions as shown in Fig. 7b. These dissociation channels are different from the abundant c-/y-ion series observed from conventional collisional activation of the $[M-2H]^{2-}$ of RNA (Fig. 7c). As demonstrated in the nET-CID data, when the oligonucleotide sequence contains multiple Gs or when the higher charge precursor ions are not available, the simultaneous activation of the survivor ions can lead to the dissociation of the oligonucleotides through channels other than those observed under CID.

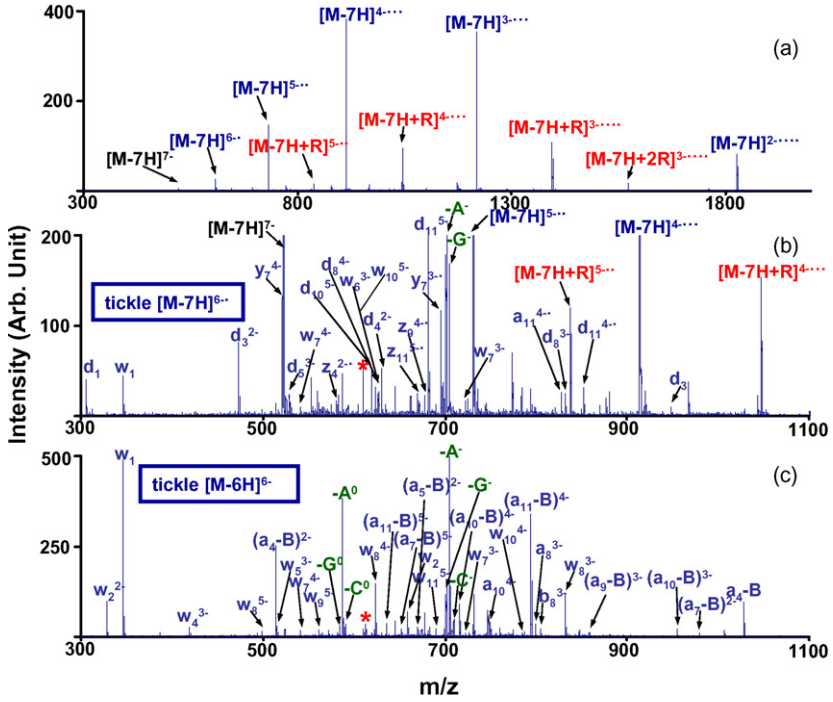

Fig. 6. Comparison of product ion spectra from (a) ion/ion reactions of the $[M-7H]^{7-}$ ions of a DNA 12-mer, dCAGAGCGCCAAG, with rubrene radical cations; (b) simultaneous activation (143 kHz, 450 mV) of the $[M-7H]^{6-\bullet}$ survivor ions during ion/ion reactions; (c) ion trap CID of the $[M-6H]^{6-}$ DNA 12-mer ions (143 kHz, 450 mV).

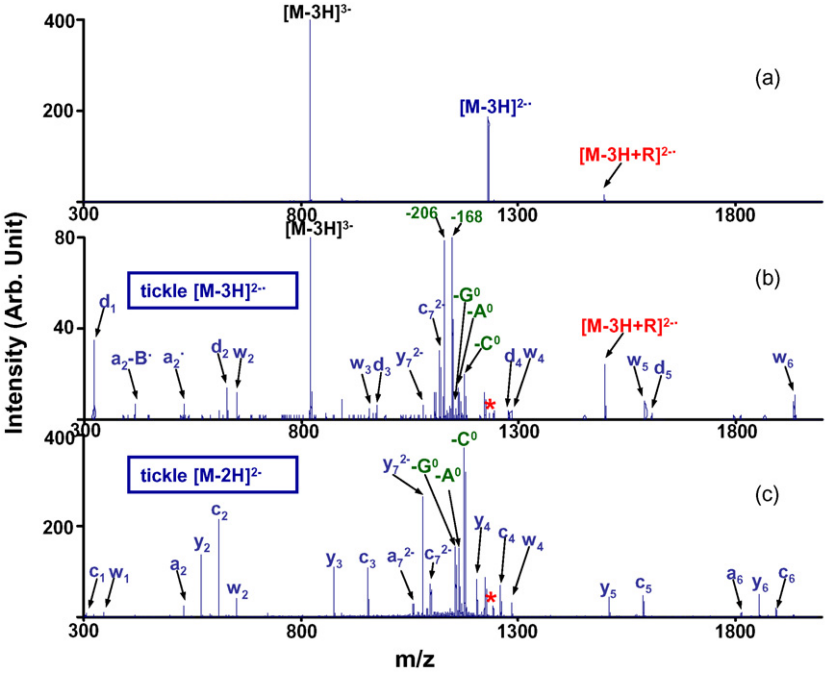

Fig. 7. Comparison of product ion spectra from (a) ion/ion reactions of the $[M-3H]^{3-}$ ions of a RNA 8-mer, rUCGCACCA, with rubrene radical cations; (b) simultaneous activation (70.5 kHz, 450 mV) of the $[M-3H]^{2-\bullet}$ survivor ions during ion/ion reactions; (c) ion trap CID of the $(M-2H)^{2-}$ RNA 8-mer ions (70.5 kHz, 450 mV).

4. Conclusions

In this study, the reaction phenomenology between multiply deprotonated DNA and RNA anions and ESI-generated rubrene radical cations has been investigated. Complex reaction channels, such as negative electron transfer without dissociation (nET, no D), complex formation and negative electron transfer dissociation (nETD) were observed for both DNA and RNA. The partitioning of the reaction channels is dependent on precursor ion charge state, oligonucleotide composition and the length of the oligonucleotides. The nETD channels were only observed when relatively highly deprotonated precursor ions were reacted. In order to improve the sequence coverage, simultaneous activation of the first generation nET, no D survivor radical anions (nET-CID) led to the generation of abundant a•/w- and d/z•-ions for sequence determination of DNA and RNA oligonucleotides. Both nETD, when observed, and nET-CID provide extensive sequence information via primarily a•/w- and d/z•-ion series. The latter ions, in particular, arise from a different backbone bond than those normally cleaved in the CID of DNA and RNA and similar to those cleaved in electron detachment dissociation and electron photodetachment dissociation. The ion/ion reaction approach provides an alternative means for accessing cleavages associated with radical anions of nucleic acid oligomers.

Acknowledgment

This research was supported by the National Science Foundation under CHE-0808380.

References

[1] B. Thomas, A.V. Akoulitchev, Trends Biochem. Sci. 31 (2006) 173.
[2] K.A. Sannes-Lowery, S.A. Hofstadler, J. Am. Soc. Mass Spectrom. 14 (2003) 825.
[3] B. Yu, Z. Yang, J. Li, S. Minakhina, M. Yang, R.W. Padgett, R. Steward, X. Chen, Science 307 (2005) 932.
[4] K.A. Kellersberger, E. Yu, G.H. Kruppa, M.M. Young, D. Fabris, Anal. Chem. 76 (2004) 2438.
[5] S.A. McLuckey, G.J. Van Berkel, G.L. Glish, J. Am. Soc. Mass Spectrom. 3 (1992) 60.
[6] J. Wu, S.A. McLuckey, Int. J. Mass Spectrom. 237 (2004) 197.
[7] K.M. Keller, J.S. Brodbelt, Anal. Biochem. 326 (2004) 200.
[8] D.P. Little, F.W. McLafferty, J. Am. Chem. Soc. 117 (1995) 6783.
[9] D.P. Little, D.J. Aaserud, G.A. Valaskovic, F.W. McLafferty, J. Am. Chem. Soc. 118 (1996) 9352.
[10] S.A. Hofstadler, K.A. Sannes-Lowery, R.H. Griffey, Anal. Chem. 71 (1999) 2067.
[11] S. Schürch, E. Bernal-Mendez, C.J. Leumann, J. Am. Soc. Mass Spectrom. 13 (2001) 936.
[12] J.M. Tromp, S. Schürch, J. Am. Soc. Mass Spectrom. 16 (2005) 1262.
[13] T.Y. Huang, A. Kharlamova, J. Liu, S.A. McLuckey, J. Am. Soc. Mass Spectrom. 19 (2008) 1832.
[14] T.Y. Huang, J. Liu, X. Liang, B.D.M. Hodges, S.A. McLuckey, Anal. Chem. 80 (2008) 8501.
[15] R.A. Zubarev, N.L. Kelleher, F.W. McLafferty, J. Am. Chem. Soc. 120 (1998) 3265.
[16] R.A. Zubarev, Mass Spectrom. Rev. 22 (2003) 57.
[17] S.D. Shi, M.E. Hemling, S.A. Carr, D.M. Horn, I. Lindh, F.W. McLafferty, Anal. Chem. 73 (2001) 19.
[18] E. Mirgorodskya, P. Roepstoff, R.A. Zubarev, Anal. Chem. 71 (1999) 4431.
[19] J.E.P. Syka, J.J. Coon, M.J. Schroeder, J. Shabanowitz, D.F. Hunt, Proc. Natl. Acad. Sci. U.S.A 101 (2004) 9528.
[20] J.J. Coon, Anal. Chem. 81 (2009) 3208.
[21] H. Han, Y. Xia, M. Yang, S.A. McLuckey, Anal. Chem. 80 (2008) 3492.
[22] H. Håkansson, R.R. Hudgins, A.G. Marshall, R.A.J. O'Hair, J. Am. Soc. Mass Spectrom. 14 (2003) 23.
[23] K.N. Schultz, K. Håkansson, Int. J. Mass Spectrom. 234 (2004) 123.
[24] S.I. Smith, J.S. Brodbelt, Int. J. Mass Spectrom. 283 (2009) 85.
[25] V. Gabelica, T. Tabarin, R. Antoine, F. Rosu, I. Compagnon, M. Broyer, E. De Pauw, P. Dugourd, Anal. Chem. 78 (2006) 6564.
[26] V. Gabelica, T. Tabarin, R. Antoine, F. Rosu, I. Compagnon, M. Broyer, E. De Pauw, P. Dugourd, J. Am. Chem. Soc. 129 (2007) 4706.
[27] J. Yang, J. Mo, J.T. Adamson, K. Håkansson, Anal. Chem. 77 (2005) 1876.
[28] J. Yang, K. Håkansson, J. Am. Soc. Mass Spectrom. 17 (2006) 1369.
[29] C. Kinet, V. Gabelica, D. Balbeur, E. De Pauw, Int. J. Mass Spectrom. 283 (2009) 206.
[30] J. Yang, K. Håkansson, Eur. J. Mass Spectrom. 15 (2009) 293.
[31] W.J. Herron, D.E. Goeringer, S.A. McLuckey, J. Am. Chem. Soc. 117 (1995) 11555.
[32] S.A. McLuckey, J.L. Stephenson, R.A.J. O'Hair, J. Am. Soc. Mass Spectrom. 8 (1997) 148.
[33] J. Wu, S.A. McLuckey, Int. J. Mass Spectrom. 228 (2003) 577.
[34] C.K. Barlow, B.D.M. Hodges, Y. Xia, R.A.J. O'Hair, S.A. McLuckey, J. Am. Soc. Mass Spectrom. 19 (2008) 281.
[35] D.M. Crizer, Y. Xia, S.A. McLuckey, J. Am. Soc. Mass Spectrom. 20 (2009) 1718.
[36] NIST Webbook, webbook.nist.gov.
[37] G.J. Van Berkel, S.A. McLuckey, G.L. Glish, Anal. Chem. 64 (1992) 1586.
[38] Y. Xia, P.A. Chrisman, D.E. Erickson, J. Liu, X. Liang, F.A. Londry, M.J. Yang, S.A. McLuckey, Anal. Chem. 78 (2006) 4146.
[39] Y. Xia, X. Liang, S.A. McLuckey, J. Am. Soc. Mass Spectrom. 16 (2005) 1750.
[40] S.A. McLuckey, T.Y. Huang, Anal. Chem. 81 (2009) 8669.
[41] Y. Xia, P.A. Chrisman, S.J. Pitteri, D.E. Erickson, S.A. McLuckey, J. Am. Chem. Soc. 128 (2006) 11792.
[42] T. Douki, J. Rivière, J. Cadet, Chem. Res. Toxicol. 15 (2002) 445.
[43] I.S. Hong, K.N. Carter, K. Sato, M.M. Greenberg, J. Am. Chem. Soc. 129 (2007) 4089.